

Calibration and Interpixel Capacitance of a H2RG(2Kx2K) Near-IR Detector

G. Smadja¹, C. Cerna² and A. Ealet²

¹IPNL, Institut de Physique Nuclaire de Lyon

4, rue Enrico Fermi, 69622, Villeurbanne cedex, France

²CPPM, Centre de Physique des Particules de Marseille

163 avenue de Luminy Case 902, 13288 marseille Cedex ,France

October 31, 2018

Abstract

A temporal analysis of the noise is performed, and non linearities are taken into account. We then extend the correlation method to groups of several pixels to derive the interpixel capacitance of a detector, found to be $x = -0.0263 \pm 0.0020$ (stat) ± 0.0040 (syst.) All measurements are consistent to a sub-percent accuracy.

1 The Apparatus

The measurements described in this paper were carried out in a dedicated setup built to evaluate Hawaii detectors H2RG from Teledyne (ex Rockwell). The detector was on loan from LBNL in view of the evaluation of its performance when used in a spectrograph for the JDEM project [1]. The cryostat can be operated in a range of temperature extending from 100K to 160K with fluctuations smaller than 0.1 K, and its equilibrium temperature in the absence of heating is about 110K. It was designed so as to ensure a variation rate of temperature smaller than 0.5 K/minute whatever the liquid Nitrogen

flow. A mirror located in the cryostat ensures a uniformity of illumination better than 1% over the full detector in the tests described in this paper.

The readout cards were adapted from the acquisition system of the OPERA neutrino experiment. Their schematic layout is shown in Figure 1, and their configuration on the cryostat in Figure 2. This acquisition system was actually used in the tests performed on the SNAP Spectrograph demonstrator in the Near infrared range [2, 3].

2 The calibration scheme

We adopt the standard method of calibration as in [4, 5] taking advantage of the stochastic Poisson fluctuations from frame to frame under illumination by a Light Emitting Diode. The overall variance will be the sum of the contributions from readout noise, common mode noise, and stochastic noise, the latter being easy to extract since it is the only one to depend on illumination. The H2RG detectors have been extensively tested in the SNAP context as reported in [6, 10]. These authors also investigated the *spatial* correlations of the signal noise. The method proposed here is a variant where the emphasis is on a *redundant* determination of the interpixel capacitance using groups of pixels, and a *temporal* analysis of the LED signal is performed, as would occur in an actual flux measurement. Non linearities are taken into account.

The ADC responds to a voltage change between two frames according to $\Delta A = k\Delta V$ where the calibration coefficient k is the product of the emitter-follower factor (0.85) and of the ADC conversion factor ($70 \mu V/9.5/ADCU$), and V is the pixel voltage.

For each LED setting, 7 to 10 consecutive measurements were performed. The first two were ignored as the detector is not in a stationary regime, and the last five were averaged to obtain our results. The spread between consecutive exposures with the same LED intensity was used to estimate the measurement errors: their origin is *NOT* statistical, *NOR* due to a slow variation of the LED intensity.

In a single pixel detector, the voltage change is linearly related (in the appropriate conditions) to the number of electron stored as $\Delta V_{pix} = q\Delta N_e/C_0$ where ΔN_e is the number of electrons stored in the pixel, q the electron charge, and C_0 the capacitance of a single pixel, quoted by Teledyne as 40ff.

The conversion factor $f_e = e/ADCU$ is then expected to be

$$f_e = \frac{\Delta N_e}{\Delta A} = \frac{C_0}{kq} \sim 2.15$$

The stochastic fluctuation of the charge on the pixel is $\delta Q = q\delta N_e$, and the variance (time average) of the ADC readouts between two frames arising from Poisson fluctuations is $\langle (\delta A)^2 \rangle = (kq/C_0)^2 \langle \delta N_e^2 \rangle = (kq/C_0)^2 \Delta N_e$. Where ΔN_e is the accumulated number of electrons between the two frames considered (to be distinguished from the fluctuation δN_e of this number).

We can substitute $\Delta N_e = \Delta Q/q = C_0\Delta V/q = C_0\Delta A/(kq)$ which yields

$$(\delta A)^2 = \frac{kq}{C_0} \Delta A = 1/f_e \Delta A \quad (1)$$

The conversion factor $f_e = e/ADCU$ is the inverse of the slope in the relation between the variance of the stochastic contribution to the noise (in ADC units) in a given time, and the flux accumulated during the same time (also in ADC units). The capacitance C_0 of the pixel can be obtained once k has been measured.

In a multipixel detector, we adopt a description close to the one proposed by [12], but more general. The charge in pixel i is now also dependent on the voltage in pixel j , and the relation is given by the electrostatic influence matrix. $\Delta Q_i = C_{ij}V_j$ (summation is implied). The ADC response in pixel i , ΔA_i will be given by:

$$\Delta A_i = kq(C)_{ij}^{-1} \Delta N_j$$

where ΔN_j is the change in the number of electrons in pixel j . The stochastic noise of pixel i can again be derived from the Poisson fluctuations in the pixels

$$(\delta_i)^2 = (kq)^2 (C)_{ij}^{-1} (C)_{il}^{-1} \delta N_j \delta N_l$$

If diffusion is negligible, there is no correlation in the numbers N_i for different pixels, and the time average of the product is $\langle \delta N_j \delta N_l \rangle = \delta_{jl} \Delta N_j$ (where δ_{jl} is the Kronecker matrix, and ΔN_j the nb of electrons collected in pixel j between consecutive frames. Using $\Delta N_j = 1/(kq)C_{jm}\Delta A_m$ we then find

$$(\delta_i)^2 = kq \sum_j (C)_{ij}^{-1} C_{ij}^{-1} C_{jm} \Delta A_m$$

So that

$$(\delta_i)^2 = kq \sum_j C_{ij}^{-2} C_{jm} \Delta A_m \quad (2)$$

This general expression will now be simplified by the use of convenient approximations of the matrices C and C^{-1} . If we consider only the coupling of adjacent pixels, with $x = C_j/C_0$ (x is negative) in a homogeneous detector, as in [4], the influence matrix C for a group of 5 pixels centered on pixel $i = 0$ as shown in Figure 3b) is $C = C_0M$, where the (5×5) matrix M is of the form

$$M = \begin{pmatrix} 1 & x & x & x & x \\ x & 1 & 0 & 0 & 0 \\ x & 0 & 1 & 0 & 0 \\ x & 0 & 0 & 1 & 0 \\ x & 0 & 0 & 0 & 1 \end{pmatrix}$$

This matrix can be inverted exactly, but as the electrostatic coupling ratio x will be found to be small, the inverse matrix can be obtained by substituting $-x$ to x when the second order terms x^2 are neglected.

We have now obtained for the single pixel noise of a homogeneous detector

$$\begin{aligned} \delta_0 &= kqC_0^{-1}\delta N_j \\ &= k\frac{q}{C_0}(\delta N_0 - x\delta N_1 - x\delta N_2 - x\delta N_3 - x\delta N_4) \end{aligned}$$

evaluating the variance from both sides of this formula, we find:

$$\langle (\delta_0)^2 \rangle = \left(\frac{kq}{C_0}\right)^2 (\Delta N_0)(1 + 4x^2)$$

As the illumination is uniform, all fluxes are equal and the mean flux in pixel $i = 0$ is $\Delta N = \frac{C_0}{kq(1-4x)}\Delta A_0 = f_e\Delta A$

$$\langle (\delta_0)^2 \rangle = \frac{kq}{C_0(1-4x)}\Delta A_0 = s_1\Delta A_0 \quad (3)$$

Under a uniform illumination, the conversion factor (e/ADCU) was however found to be

$$f_e = \frac{\Delta N}{\Delta A} = \frac{C_0}{kq(1-4x)}$$

so that

$$f_e = \frac{1}{s_1(1-4x)^2} \quad (4)$$

As x is negative, the conversion factor will now be smaller than the inverse of the slope, and smaller than expected for a 'single pixel'. The edge effect

from adjacent pixels is expected to decrease for larger groups of pixels, and the relation between slope and conversion factor should be closer to the single pixel case.

3 Noise fluctuations for groups of pixels

The previous formulae allow us to measure the ratio $x = C_i/C_0$ by comparing the relation between noise and flux for groups of pixels, as this changes the weight of the contribution of the neighbouring pixels.

2 pixel groups (as shown in Figure 3a)

The 8×8 capacitance matrix C to be considered follows from Fig. 3 a):

$$C = \begin{pmatrix} 1 & x & 0 & 0 & 0 & x & x & x \\ x & 1 & x & x & x & 0 & 0 & 0 \\ 0 & x & 1 & 0 & 0 & 0 & 0 & x \\ 0 & x & 0 & 1 & 0 & 0 & 0 & 0 \\ 0 & x & 0 & 0 & 1 & x & 0 & 0 \\ x & 0 & 0 & 0 & x & 1 & 0 & 0 \\ x & 0 & 0 & 0 & 0 & 0 & 1 & 0 \\ x & 0 & x & 0 & 0 & 0 & 0 & 1 \end{pmatrix}$$

For a typical value of $x = -0.02$, the diagonal elements of the inverse matrix vary from 1.0004 to 1.0016, while the off-diagonal elements of adjacent pixels differ from 0.02 by less than $5 \cdot 10^{-5}$, the other coefficients are smaller than $4 \cdot 10^{-4}$. Neglecting all small offsets, we find:

$$\begin{aligned} \delta_2 &= \frac{1}{C_0}(\delta Q_1(1-x) + \delta Q_2(1-x) \\ &\quad - x \sum_{i=3, i=8} \delta Q_i) \\ (\delta_2)^2 &= \left(\frac{k\delta Q}{C_0^2}\right)^2(2 - 4x + 8x^2) \sim \left(\frac{kq}{C_0}\right)^2 \Delta N \end{aligned}$$

and substituting for the expression of ΔN_0 in terms of the observed ADC shift ΔA_0 in 1 pixel between frames

$$\Delta N_0 = \frac{C_0}{kq(1-4x)} \Delta A_0$$

$$(\delta_2)^2 = 2 \frac{kq}{C_0(1-4x)} (1-2x+4x^2) \Delta A_0 \quad (5)$$

5 pixel groups (Figure 3b)

We find in the same way:

$$\delta_5 = \frac{1}{C_0} (\delta Q_0(1-4x) + (1-x) \sum_{i=1,4} \delta Q_i - 2x \sum_{i=5,8} \delta Q_i - x \sum_{i=9,12} \delta Q_i)$$

So that

$$(\delta_5)^2 = \left(\frac{k\delta Q}{C_0} \right)^2 (5-16x+40x^2) \sim \left(\frac{kq}{C_0} \right)^2 \Delta N_0 (5-16x)$$

and using as before the relation between ΔN_0 and ΔA_0 , the ADC shift:

$$(\delta_5)^2 = \left(\frac{kq}{C_0} \right)^2 \frac{5-16x+40x^2}{1-4x} \Delta A_0 \quad (6)$$

9 pixel groups (Figure 3c)

and for 9 pixels forming a (3×3) square (see Figure 3):

$$\delta_9 = \frac{k}{C_0} (\delta Q_0(1-4x) + (1-3x) \sum_{i=1,7(odd)} \delta Q_i + (1-2x) \sum_{i=2,8(even)} \delta Q_i - x \sum_{9,20} \delta Q_i)$$

$$(\delta_9)^2 = \left(\frac{k\delta Q}{C_0} \right)^2 (9-48x+80x^2) \Delta N$$

$$\delta_9^2 = \frac{kq}{C_0} \frac{9-48x+80x^2}{1-4x} \Delta A_0 \quad (7)$$

4 The measurement method

The cryostat temperature was set at 110K, the equilibrium value in the absence of any heating, during these tests. In contrast with previous publications, which used the spatial correlations under different illumination conditions ([7]), we have used the time variation of the signal to evaluate the noise and the correlation, as a training for the flux measurements anticipated in the near future. The frames are grouped into 'bursts', the number of frames

in each burst decreasing from 60 (LED current of $10 \mu\text{A}$), to 15 (LED current of $100 \mu\text{A}$). The variance of the differences of readouts for consecutive frames is then evaluated for each pixel, and each burst, and the measurement is repeated 'up the ramp' until saturation is reached. The results are then averaged over all pixels for each burst. At any LED setting at least 10 exposures are taken to allow control of the error estimates.

4.1 Non-linearities

The distribution of the flux in ADC units averaged over all bursts for all pixels at a typical setting with a LED current of $40 \mu\text{A}$ is shown in Figure 4 a). It is seen that in the absence of flatfielding corrections, its spread is 3.5%. This good homogeneity of the detector in the analysis window allows averaging of the measured properties over all pixels (the flux and variance of each pixel is still evaluated independently). A linear variation of $dADC/dt$ and of the single pixel noise along the ramp is then observed in Figure 4 b). As the flux measurement is perfectly reproduced from one exposure to the next, the flux variation is an indication of the non-linear response of the system. The most likely source of this behaviour is the output FET, and the observations suggest a decrease of the transconductance as the grid voltage decreases with an increasing number of trapped electrons in the pixel well. The slopes of the variance and of the flux (normalised to their value at an output ADC value of 19000 ADCU) are respectively $a_{var} = 0.000388$ and $a_{flux} = -0.000336$, and they correspond to similar (and opposite) relative variations, as expected if the equivalent thermal resistor is the inverse of the transconductance. The effective conversion factor given by the ratio variance/flux cannot be obtained without further corrections. All the following analyses have been performed with 2 different extrapolations, namely to the middle (32500) and to the lower values (10000) of the ADC dynamical range. To crosscheck the validity of the corrections, different LED illuminations will be compared. The conversion factors found are expected to differ by 5% as a consequence of the non linear response, but the interpixel capacitance obtained should be the same up to systematic errors.

4.2 The 2 pixel pairs

It is instructive to consider separately horizontal (readout direction) and vertical pairs of pixels. Horizontal pairs are read consecutively, while vertical

Table 1: Readout Noise Horiz./Vert. pairs

Pixel group	var(ADCU)
1	121.02± 0.77
2-H	249.17± 1.50
2-V	261.24± 1.79

pairs are separated by the time interval needed to complete the readout of the intermediate pixels. The variance quoted in Table 1 is obtained in the absence of any illumination by summing 2 pixels, measuring the difference between consecutive frames, estimating its variance for each burst (of typically 60 frames), averaging over all bursts, and then over all pairs. The result for the mean variance is given.

It is seen that intrinsic voltage changes in the chip during the readout impact the variance a level of about 4%. Analyse is in progress to shown soon results including a temporal common mode correction by subtracting a reference channel.

4.3 The 5 and 9 pixel configurations

The measured values of the variance and the flux for each pixel grouping is shown in figure 5 for 12 illumination conditions. The expected linear relation (after correcting for the non-linear response!) is observed in Figure 5 for the data and the slopes found from the extrapolation to lower flux values are given in Table 2.

The ratio x of the interpixel capacitance to the pixel capacitance C_0 is found from the comparison of the slopes for 1,2,5,and 9 pixels: To modify the impact of the fluctuations from adjacent pixels, we now evaluate their contribution to the variance of larger groups of pixels. The interpixel capacitance $x = C_c/C_0$ can then be derived for each pixel grouping from equations (5),(6),(7).

Table 2: slopes

pixel group	Slope
1	0.4021 ± 0.0026
2	0.8458 ± 0.0049
5	2.2139 ± 0.0218
9	4.2095 ± 0.0550

4.4 Conversion factor and effective Interpixel capacitance

The values of the interpixel capacitance found in all cases are given in Table 3 with the linearity correction extrapolated to the lower ADC range (10000). They are compatible, with small residual systematic shifts, and we shall perform a weighted average.

Table 3: The Slope ratios and Interpixel capacitance

Group	ratio	x
s2/s1	2.1028 ± 0.0183	-0.02455 ± 0.00416
s5/s1	5.5063 ± 0.0651	-0.02947 ± 0.00352
s9/s1	10.4696 ± 0.1529	-0.02916 ± 0.0029

$$x = -0.0282 \pm 0.0020$$

The value $x = -0.0282 \pm 0.0020$. The same averages performed at ADCU = 30000 leads to $x = -0.02440 \pm 0.001$ For our final result, we take the average of the two estimates and attribute a systematic error of 0.0040 to account for the small difference in the non-linearity corrections (mid range and low range).

$$x = \frac{C_{int}}{C_0} = -0.0263 \pm 0.0020(\text{stat}) \pm 0.0040(\text{syst})$$

The (single pixel) conversion factor in the lower ADC range can now be obtained as

$$f_1 = \frac{\Delta Q_0}{\Delta ADC_0} = \frac{1}{s_1(1 - 4x)^2}$$

$$= \frac{2.487}{(1 - 4x)^2} = \frac{2.487}{1.221} = 2.036(e/ADCU)$$

and it is 10% larger at full well. The conversion factors found in the 2 extrapolation methods differ by 5%, as expected from the nonlinear behaviour seen in figure 4b): they are evaluated at different values of the ADC range. The result is very close indeed to the value of 2.15 derived from an assumed pixel capacitance of 40ff in section 2.

4.5 Diffusion and actual Interpixel capacitance

The effective value of the interpixel capacitance found would *NOT* be the true value if 'fast' diffusion would occur as suggested by [6]: while the interpixel capacitance increases the fluctuations, diffusion from one pixel to the adjacent ones would reduce them. A detailed computation shows that the contribution to x_d from diffusion is equal to the fraction f_d of electrons migrating to the adjacent pixel for 2 and 5 pixel groups, but is only $x_d = f_d/3$ for the 9 pixel group. Given the consistency of the previous results between 9 and 5 pixel groups, we obtain $f_d < 0.037$ (3 σ limit).

5 Conclusions

A general correlation method has been proposed, which allows strong cross-checks for internal consistency of the observations between different pixel groups. We have shown that the non-linearities which are seen are consistent with the effect of a transconductance variation in the output FET of the detector, and that they can be corrected to a sub-percent accuracy. The remaining systematic errors are in the 10^{-3} range. It has also been shown that the use of the reference channel have to be studied in that frame of work. The impact of that studies will be shown in a forthcoming paper. The calibration of the readout set-up will be studied in order to describe the noise performance achieved under different conditions.

6 Acknowledgements

We thank all the institutions who have supported us during this work: Université Claude Bernard Lyon 1, The IN2P3/CNRS institute, and the engineers and technicians at IPNL and CPPM who have contributed to the

apparatus JC Ianigro, A. Castera, and in particular C. Girerd who has designed the readout electronics. We are indebted to C. Bebek (LBNL) for lending us the H2RG detector, and to G. Tarle, M. Schubnell, and R. Smith for many questions and suggestions.

References

- [1] M.-H. Aumeunier et al. Proc. SPIE 6265,626534 (2006) *An integral Field Spectrograph Demonstrator based on a slicer*
- [2] C. Cerna et al. Proc. SPIE Vol. 7010,7010A(2008);DOI:10.1117/12.789583 *Setup and performance of the SNAP spectrograph Demonstrator*
- [3] M-H. Aumeunier et al. Proc. SPIE Vol. 7010, 70103N(2008);DOI:10.1117/12.789587 *First results for the spectrophotometric calibration of the SNAP spectrograph Demonstrator in the visible range*
- [4] G. Finger et al. *Performance Evaluation and calibration issues of large Format Infrared Hybrid active pixel sensors (NIM A Vol. 565,1 (Sept 2006)2008*
- [5] G. Finger et al. *Performance Evaluation,readout modes, and calibration techniques of HgCdTe Hawaii-2RG mosaic arrays SPIE2008,Marseille*
- [6] N. Barron, M. Borysow, K. Beyerlein, M. Brown, C. Weaverdyck, W. Lorenzon, M. Schubnell, G. Tarl and A. Tomasch Proceedings of the Astronomical Society of the Pacific 119, 466-475,2007 *Sub-Pixel Response Measurement of Near-Infrared Sensors*
- [7] M. Brown,M. Schubnell, G. Tarlé PASP 118:1443-1447,2006 *Correlated Noise and Gain in Unfilled and Epoxy-Underfilled Hybridized HgCdTe Detectors Sub-Pixel Response Measurement of Near-Infrared Sensors*
- [8] M.G. Brown, et al., Proc. SPIE Vol. 6265, 626535 (2006). *Development of NIR Detectors and Science Driven Requirements for SNAP*
- [9] M. Schubnell, et al. Proc. SPIE Vol. 6276, 62760Q (2006).

- [10] R. Smith, et al., Proc. SPIE Vol. 6276, 62760R (2006) *Noise and Zero Point Drift in 1.7 μ m Cutoff Detectors for SNAP*
Near Infrared Detectors for SNAP
- [11] S. Seshadri, et al. Proc. SPIE Vol. 6276, 62760S (2006). *Characterization of NIR InGaAs Imager Arrays for the JDEM SNAP Mission Concept*
- [12] P. R. McCullough et al. PASP 120:759-776, July 2008 *Quantum Efficiency and Quantum yield of an HgCdTe Infrared Sensor Array*

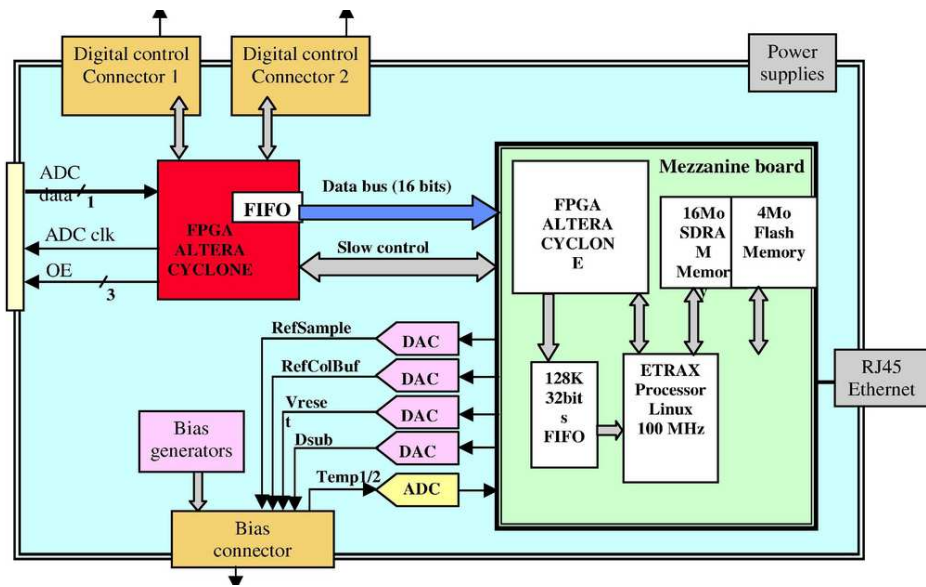


Figure 1: Scheme of the acquisition card

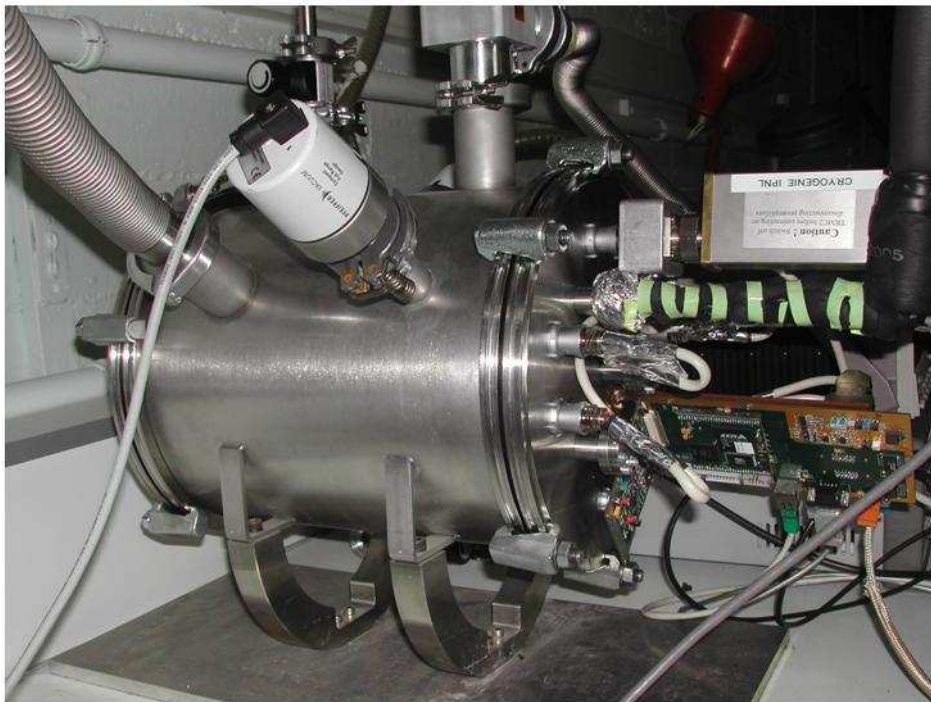
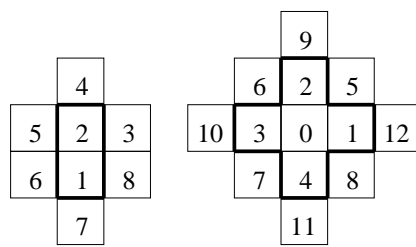


Figure 2: Cryostat with the readout cards



a)

b)

	14	13	12	
15	4	3	2	11
16	5	0	1	10
17	6	7	8	9
	18	19	20	

c)

Figure 3: Map of the 2, 5, and 9 pixels groups

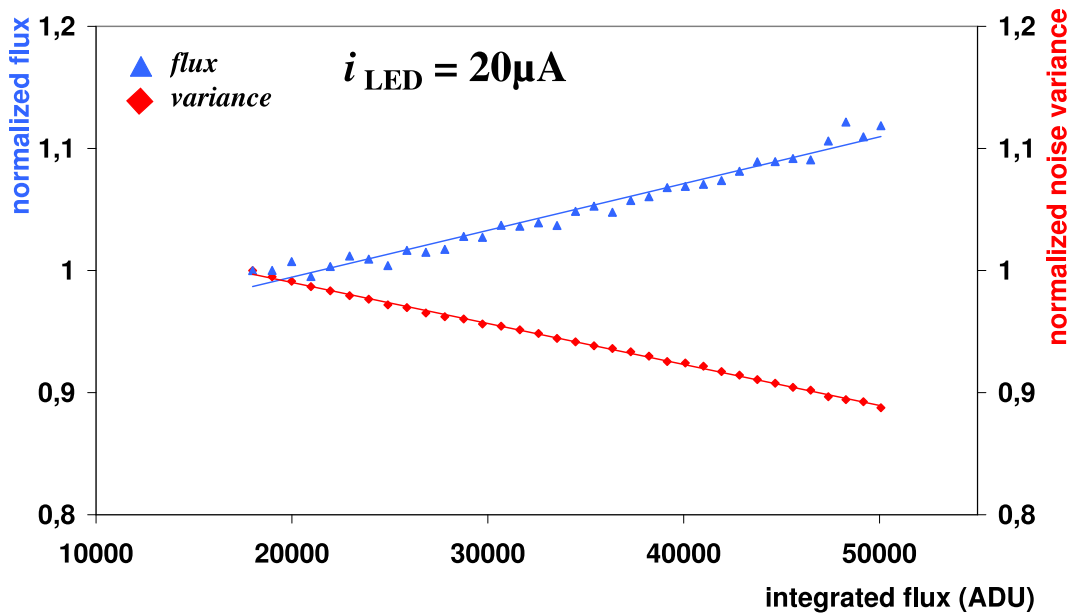
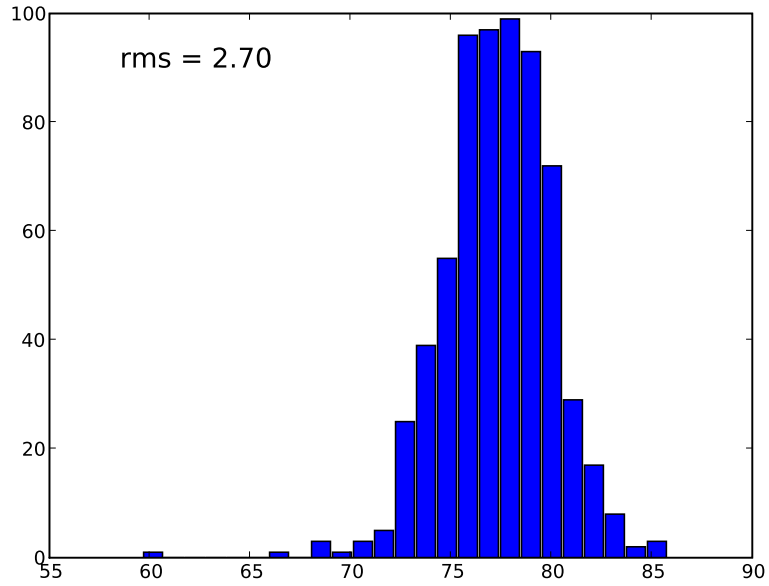


Figure 4: a) flux distribution ADCU/pixel/frame for an LED setting at $40 \mu\text{A}$ b) variance $(\text{ADCU})^2$ and flux (ADCU) as a function of the ADC value, for a LED setting at $20 \mu\text{A}$.

H2RG #40 Variance of noise versus measured flux

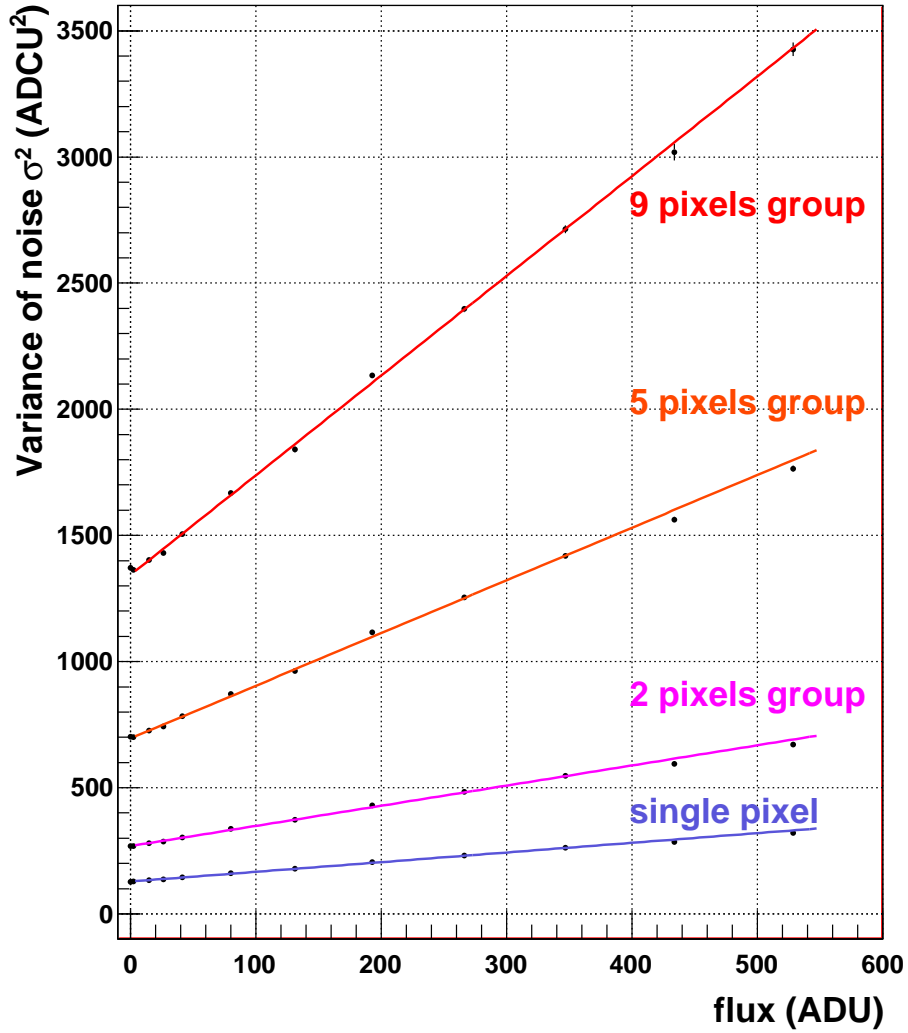


Figure 5: noise(without reference subtraction)/Flux for single pixels and groups of 2,5 and 9 pixels